UNIVERSITY OF CALIFORNIA SAN DIEGO

Investigation of *Chaetopterus variopedatus* Mucus Bioluminescence Utilizing Cofactor Fe^{2+} and other Metal Ions

A thesis submitted in partial satisfaction of the requirements
for the degree Master of Science

in

Marine Biology

by

Tianyun Hua

Committee in charge:

Dimitri D. Deheyn, Chair
William Gerwick
Nicholas Holland

2020

The thesis of Tianyun Hua is approved, and it is acceptable in quality and form for publication on microfilm and electronically:

_____

_____

_____

Chair

University of California San Diego

2020

DEDICATION

This thesis is dedicated to my mother Weiping Wu, together with my father Dong Hua. For they have taught me how to grow as a person, encouraged me when during my times of darkness, and provided me with priceless advice when I'm lost and confused. I would like to also dedicate this thesis to my advisor Dimitri Deheyn and my lab members who have always been there for me.

EPIGRAPH

In the ocean, bioluminescence is the rule rather than the exception.

Edith Widder

TABLE OF CONTENTS

LIST OF FIGURES

LIST OF TABLES

LIST OF ABBREVIATIONS

cDNA: complementary deoxyribonucleic acid

ChF: *Chaetopterus* Ferritin

E. coli: *Escherichia coli*

FPLC: Fast Protein Liquid Chromatography

IPTG: isopropyl β-D-1-thiogalactopyranoside

LB: lysogeny broth

LCR: light change ratio

MES: 2-(N-morpholino) ethane sulfonic acid

MOPS: 3-morpholinopropane-1-sulfonic acid

mQ: milliQ ultrapure water

PAGE: polyacrylamide gel electrophoresis

Redox: reduction-oxidation

RNA: ribonucleic acid

ROS: reactive oxygen species

rpm: revolutions per minute

SDS: sodium dodecyl sulfate

UV: ultraviolet

ACKNOWLEDGEMENTS

First of all, I would like to thank my advisor, Dimitri Deheyn, PhD. I cannot express how grateful I am to have the opportunity to work in the lab for almost three years. Thank you for accepting me into the lab in the first place and introducing me to the fantastic realm of marine bioluminescence. I appreciate all the inspirations that you have given me while I'm stuck in my learning process. You have so much confidence in me and always showed great appreciation which means a lot to me. Your endless, brilliant ideas have taught me how to think as a scientist and explore like an adventurer.

Next, I would like to express deep gratitude to my mentor Evelien De Meulenaere, PhD. Thank you for not only teaching me all the valuable lab skills from simple pipetting to using the exquisite FPLC machine, but also training me to think independently like a scientist by putting me into the real world of science. Moreover, thank you for helping me revise the writings and poster that I have done ever since I first came into our lab. I deeply appreciate the precious time that you spent on helping me perfect down to the tiniest detail. Thank you for being my mentor not only in science but also in life, for passing your knowledge without reservation, and for making my projects possible.

I would like to express my gratitude to Professor Nicholas Holland and Professor William Gerwick for giving me the opportunity to have you on my committee. Thank you for meeting with me even when you're very busy and inspiring me with brilliant ideas.

I would like to recognize Phil Zerofski for collecting the *Chaetopterus variopedatus* samples from La Jolla Canyon, my project would not be able to proceed without your help.

I would also like to thank all my lab members. Especially our lab manager Michael Allen for being extremely patient in teaching me how to use the equipment in lab and helping me push through obstacles in life. Your kindness meant a lot to me. Thank you, Kelly, for warming my heart whenever I feel down, for listening to my nonsense and being supportive all the time. Thank you, Laura, for inspiring me with your passion for science and teaching me what selfless, true friendship is like.

Last but not least, I want to express gratitude to my family. Thank you, my Mom and Dad, for supporting me and being there for me all this time. I would never have gone this far without your love. I also want to thank Bofu for spending so much time patiently helping me with MATLAB coding figures and analyzing data. Thank you for putting up with all my nonsense and loving me for who I am.

ABSTRACT OF THE THESIS

Investigation of *Chaetopterus variopedatus* Mucus Bioluminescence Utilizing Cofactor Fe^{2+} and other Metal Ions

by

Tianyun Hua

Master of Science in Marine Biology

University of California San Diego, 2020

Dimitri D. Deheyn, Chair

The photoprotein of marine polychaete, *Chaetopterus variopedatus,* has been under investigation for decades because of its unique long-lasting light production ability and the potential of utilization in biochemical research as a reporter molecule. However, the exact light-producing mechanism remains unknown except that Fe^{2+} acts as the cofactor for the photoprotein. The goal of this thesis is to investigate this bioluminescence reaction pathway and to hopefully extract the previously unknown photoprotein. we discovered a preliminary relationship between

Fe^{2+} (photoprotein cofactor) concentration and mucus bioluminescence—a stimulation-inhibition dose response curve where ferrous iron stimulates light at a low concentration (≤ 0.1 mM added) and starts to inhibit light as concentration increases (> 0.1 mM). Evidence suggests that Co^{2+} and Zn^{2+} are both competitive inhibitors for binding to the cofactor site on photoprotein and for bioluminescence. Co^{2+} has a stronger affinity than Fe^{2+} while Zn^{2+} has a lower affinity compared to Fe^{2+}. We were able to purify Fe^{2+} binding protein from the mucus complex using Fe^{2+}-affinity column. By using Co^{2+} as a substitute cofactor, we extracted from the mucus a light-inducing protein (37 kDa), which is a potential candidate for photoprotein or a protein that plays a role in the light production pathway.

Introduction

This thesis aimed at deciphering the process of light production from the marine worm *Chaetopterus variopedatus*. The light production originates from mucus the worm secretes in the surrounding seawater and the bioluminescence, in contrast to other systems, occurs for a long time. The energy source supporting the light production, and the chemical process of light production (the chromophore identity), remain unknown to this day. My thesis was therefore to fill in this gap.

Chaetopterus variopedatus: an unusual light producing worm

Chaetopterus variopedatus is a tube-dwelling, filter-feeding marine parchment tubeworm that has a world-wide distribution from sandy bottom in canyons on continental shelves coastal to shallow waters (Shah *et al*. 2015). Individuals burrow in sand and produce a U-shaped tube with narrowed opening on both sides to dwell themselves (Figure 1). They lead a sedentary style of life and rely on the circulation of sea water through the tube to bring food particles (Enders, 1905). The worm has a sophisticatedly segmented and differentiated body. The head region alone is divided into 11 segments (H in Figure 2A) with a funnel-shaped mouth at one end. The 12th segment is also known as the aliform parapodia (AP), which contains large amounts of mucus-producing cells—mucocytes. Posterior sections includes circular fan-like structures (CP in Figure 2A) to facilitate water circulation inside of the tube and sexual segments (T) that contain male/female reproductive cells (Berrill, 1928). Macginitie (1939) demonstrates that while feeding, the worm is able to secrete mucus from the aliform parapodia to form a bag which traps detritus (organic debris and bacteria) in the flowing water while the fans maintain the current. Ultimately a bolus of food is rolled up and swallowed through the buccal funnel.

Ever since the 19th century, it was observed that *C. variopedatus* individuals exhibit blue light on their epithelia upon mechanical stimulation, with a continuous spectrum from 440 to 530 nm (Lankester, 1868). Interestingly, the aliform parapodia also have photogenic glands that renders luminescence to the secreted mucus into the environment, while in other regions, light production is localized on the worm body (Nicol, 1952). Nicol (1962) hypothesizes that the luminescence produced is aimed to drive out the intruders in the tube, such as small crustaceans. Others postulate that the luminescence might serve as prey attraction and/or predator deterrence (MacGinitie 1939). What's most intriguing about the extracellular secretion is that it does not just emit an ephemeral flash, but a long-lasting glow—Rawat and Deheyn discovered in 2016 that the mucus on its own can produce light for more than 15 hours.

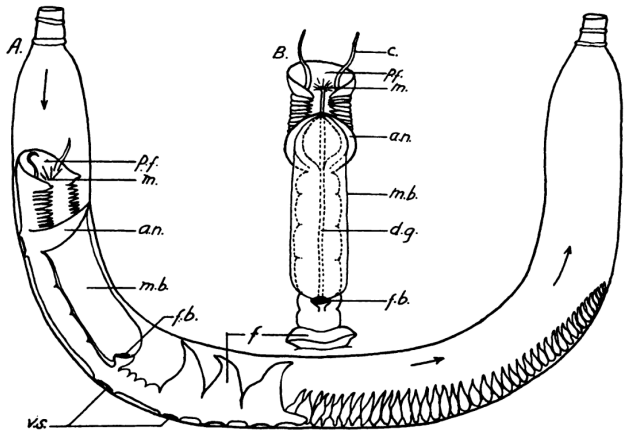

Figure 1. Drawing of *Chaetopterus variopedatus* within its tube (Macginitie, 1939).

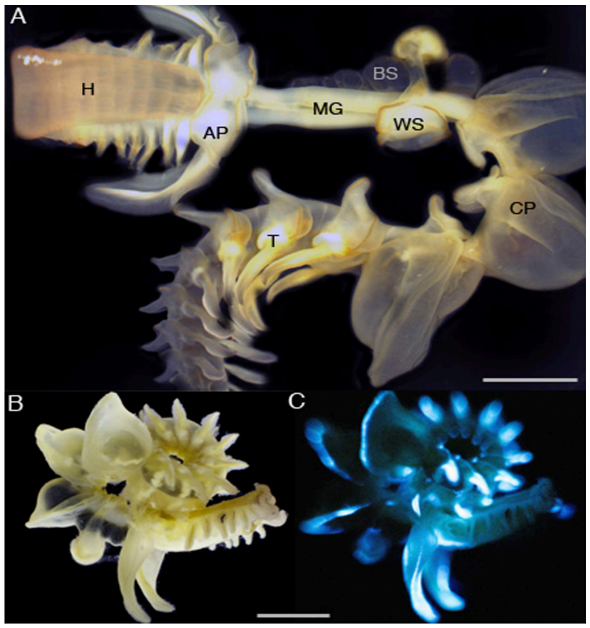

Figure 2. *Chaetopterus variopedatus* body parts, AP: aliform parapodia. (A), worm in bright field (B), and the worm while producing blue light upon KCl injection (C). Picture B, C courtesy of David Littschwager (Rawat, R., & Deheyn, D. D., 2016).

Bioluminescence: fundamental chemical properties

Bioluminescence refers to the ability of a living organism to produce light utilizing biochemical pathways. It is an adaptation that has independently evolved to become extremely diverse in the marine environment—occurring in a wide range of marine organism from bacteria to vertebrates, all with their own modified version of light production mechanism. The most abundant bioluminescent species were found in the comb jellyfish phylum (Haddock *et al*., 2010). Since it has evolved in the open ocean, the most common light emission locates in the blue region of visible light, which travels the farthest in the sea (Archer *et al.,* 2013). There are mainly three proposed ecological functions that bioluminescence serves in the marine environment. Firstly, predators in the dark environment of deep sea can utilize light production to locate food sources

and preys. Secondly, organisms can use bioluminescence as a way of communication to find and attract potential mates where encounter is difficult without light. Thirdly, preys exhibit bioluminescence to deter predators by shocking, blinding them or mark them visible for secondary predators (Archer *et al.,* 2013).

The general reaction mechanism of bioluminescence is the oxidation of luciferin (substrate) by molecular oxygen catalyzed by luciferase (enzyme) (Figure 3). Reaction energy is contained in a transient product for a short amount of time and then released in the form of photon (Wilson & Hastings, 1998). Although the light emission seems to be a simple reaction, luciferases and luciferins in different marine organisms evolved independently. Not to mention that the enzyme luciferase comes in great diversity in terms of amino acid sequence, even the luciferins are found to be completely different small molecules. Luciferin is a common term that encompasses many different chemical compounds; one organism can have its own unique luciferin while another luciferin can be found in multiple species of organisms, then likely related to the diet. For example, most common luciferins are bacterial luciferin (proper to bacteria) that are found either in free living or in symbionts; *Cypridina* luciferin are found specifically in ostracods, dinoflagellate luciferin is found in dinoflagellates but also euphausiids, while coelenterazine is a common luciferin found in a wide range of organisms (Widder, 2010). In the meantime, new light production processes have always been explored and discovered.

In 1962, from the tissue of *Aequorea victoria* (a marine hydrozoan jellyfish), Shimomura *et al.* isolated aequorin, a luminescent protein which only requires the addition of Ca^{2+} to produce light. The presence of oxygen as a reactant in the light production step is not required in this case. They later named the light producing protein "photoprotein". Diverging from the classic

luciferase-luciferin model where the presence of molecular oxygen is required, the luminescence system of a photoprotein is where the enzyme binds oxygen and luciferin in advance to form a pre-oxidized complex. This complex produces bioluminescence in absence of oxygen and requires solely the cofactor to trigger light (Shimomura, 1985). Several Ca^{2+}-activated photoproteins—halistaurin, phialidin and obelin—were discovered in three other marine hydromedusan species. There are also systems that require activation from other cofactors. For example, the photoprotein found in a terrestrial millipede, *Luminodesmus*, requires Mg^{2+} and ATP to produce bioluminescence (Shimomura, 1981).

Discovering new photoproteins and understanding their reaction mechanism can be of great value to biological research. They are excellent candidates for luminescent labels in binding assays because of the fact that the luminescence can be triggered solely by the metal cofactor, which will produce little to no background (Lewis & Daunert, 2000). This can serve as a fundamental reporter protein system in biological research wherever protein expression is conducted. Aequorin was used as a biological assay to determine Ca^{2+} concentration in a variety of environments, including not only extracellular fluid, but also intracellular organelles and muscle fibers (Blinks *et al.*, 1976). In our case, discovering the Fe^{2+}-binding photoprotein from the worm mucus gives us a possibility to develop an assay that can use luminescence levels to quantify the amount of Fe^{2+}, which is also an essential element in biological systems as well as the marine environment.

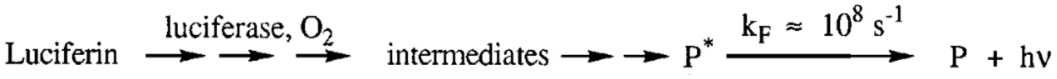

Figure 3. General reaction mechanism of bioluminescence. P*, the transient product holding reaction energy. P, product; hv, releasing of photon (Wilson & Hastings, 1998).

The unique bioluminescence aspects from Chaetopterus variopedatus

In 1966, Shimomura proposed that *C. variopedatus* is also utilizing a photoprotein system to generate light and the cofactor is Fe^{2+}. This conclusion was further confirmed by Deheyn *et al.* (2013) that, contrary to the luciferin-luciferase system, the light producing mechanism of the worm's mucus does not require the presence molecular oxygen to trigger the reaction.

Based on previous research, the emphasis of investigating photoprotein lies in the cofactor. According to Rawat and Deheyn (2016), both ferrous and ferric ion are present in the mucus complex; the concentration of Fe^{2+} in the mucus is around 2.41×10^{-5} to 8.76×10^{-3} mM. Due to the fast oxidation of Fe^{2+} in sea water, there must be a protein that's maintaining the supply of ferrous iron as the cofactor of bioluminescence in the mucus. It was demonstrated that the concentration of a ferroxidase protein, ferritin, is directly proportional to the intensity of chemiluminescence (Rawat & Deheyn, 2016). Ferritin consists of 24 subunits (Granick, 1946), forming a spherical cage with 8 channels providing entry for Fe^{2+} /Fe^{3+} (Desideri, 1991). Free Fe^{2+} is taken up by ferritin, oxidized and stored in the ferroxidase center in the form of Fe^{3+} mineral core. Biologically relevant reducing reagents, such as dihydroflavins, are required in order for ferritin to release iron in the form of Fe^{2+} (Jones *et al.*, 1978).

In this project, we will focus on testing mucus bioluminescence utilizing Co^{2+} and Zn^{2+} as well as using chromatography to fish out potential components that are involved in the reaction chain. Previous hypothesis proposed in 2016 includes two possible directions—firstly, ferritin is a steady source of Fe^{2+} cofactor to activate the photoprotein. Secondly, ferritin can be driving a complex oxidation-reduction reaction chain involving multiple other components (including FMN and NADH), which generates electron spin that directly provide energy to excite the chromophore

inside of the photoprotein (Figure 4). In order to better understand the reaction, we can use other metal ions to explore and hopefully elucidate the reaction chain through the effect that they have on photoprotein and ferritin. Zn^{2+} is long known to be the inhibitor of ferritin because it blocks ferrous irons' access to the ferroxidase center (Bou-Abdallah *et al*., 2003) while Co^{2+} can have the same redox reaction with ferritin compared to Fe^{2+} (Douglas & Stark, 2000). Affinity chromatography is a useful technique that is applied in our searching of proteins participating in the bioluminescence. The basic principle is to first immobilize an interacting ligand in the reaction to the immobile phase (such as sepharose beads) on a column, and then flow the mixture of protein in the mobile phase (buffer) through the immobile phase—any protein that interacts with the ligand will stay on the column beads. Afterwards, the bound protein can be eluted by buffer containing high concentration of binding competitor that will compete binding to the ligand with the desired protein (Chang *et al.,* 2017*)*. This way the targeted protein is extracted and collected in fractions.

Discovering new photoproteins and understanding their reaction mechanism can be of great value to biological research. They are excellent candidates for luminescent labels in binding assays because the luminescence can be triggered solely by the metal cofactor, which will produce little to no background (Lewis & Daunert, 2000). This can serve as a fundamental reporter protein system in biological research wherever protein expression is conducted. Aequorin was used as a biological assay to determine Ca^{2+} concentration in a variety of environments, including not only extracellular fluid, but also intracellular organelles and muscle fibers (Blinks *et al.*, 1976). In our case, discovering the Fe^{2+}-binding photoprotein from the worm mucus gives us a possibility to develop an assay that can use luminescence levels to quantify the amount of Fe^{2+}, which is also an essential element in biological systems as well as the marine environment.

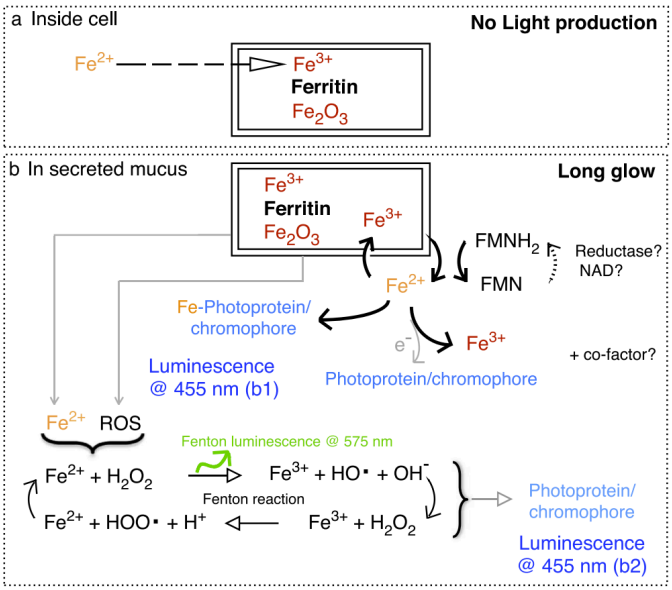

Figure 4. Schematic representations of different hypotheses of *C. variopedatus* bioluminescence mechanism (Rawat & Deheyn, 2016).

Here, we discovered a preliminary model of the relationship between Fe^{2+} concentration and mucus bioluminescence, which exhibits a stimulation-inhibition dose response curve. We also tested the hypothesis that the electron spin from the oxidation-reduction chain involving ferritin will excite the chromophore inside of the photoprotein by using Zn^{2+} and Co^{2+}.We were able to elucidate the interaction between these two metal ions and the reaction pathway. Furthermore, our attempt to extract light-inducing fraction from the mucus using Co^{2+}-affinity column was successful.

Materials and Methods

Worm collection

Chaetopterus variopedatus colonies (bundles of tubes) were collected from the La Jolla submarine canyon at around 23 m deep and kept in open running sea water tanks inside of the experimental aquarium (Marine Biology Research Division of Scripps Institution of

Oceanography). The water was a mix of circulating ambient and chilled sea water; the worms were not fed, counting on them being able to get nutrients from the running sea water.

Luminous mucus extraction

A *Chaetopterus* individual was removed from its parchment tube and placed onto a plastic reservoir on ice without sea water (collected mucus was not diluted). The worm was gently agitated mechanically with a plastic pipette tip. Mucus secreted (mostly from the head region and 12th segment) was collected over the 30-40 min of the process. When multiple individuals were utilized, mucus samples were pooled together. No chemicals were used to make the collection of mucus, and the worm was kept alive through the entire process. In fact, most times, live worms were placed back into the seawater tanks in the aquarium for analysis another time.

Recombinant Chaetopterus ferritin purification.

In order to isolate ferritin and test its activity aside from the mucus complex, it is necessary to express the gene in bacteria and isolate the protein. The *C. variopedatus* ferritin (ChF) gene was originally acquired from RNA and cDNA cloned into a pET24b expression vector (Invitrogen) using the forward primer (CACAAGATCATATGGCCCAGACTCAGCCG) and the reverse primer (GTCGTGGATCCTTAGCTGCTCAGGCTCTCCTTGT). Plasmid was transformed into a BL21 star^{TM} *Escherichia.coli (E.coli*) cells (Invitrogen) to grow overnight at 37 °C on Kanamycin plate. Cell cultures were grown in liquid lysogeny broth (LB) culture containing 1 mM Kanamycin until optical density at 600 nm reached 0.7-0.8 nm, and recombinant protein was

expressed for 15 h after induction with isopropyl β-D-1-thiogalactopyranoside (IPTG). *E. coli* cells were harvested by centrifugation at 4 °C at a speed of 4,000 ×g for 25 min.

Pellets were resuspended in 25 mM Tris buffer containing 200 mM NaCl at pH 7 and lysed with lysozyme and benzonase® nuclease for 30 min each at 37 °C. The suspension was then sonicated on ice with a needle sonicator for 6 min with an interval of 0.5 s, and centrifuged at 11,000 rpm for 15 min at 4 °C. The supernatant was transferred into a new tube and heat shocked in a water bath at 75 °C for 15-20 min, and centrifuged at 11,000 rpm for 15 min at 4 °C.

The supernatant obtained was further purified by running through 15 mL Hi-trap Q column in Fast Protein Liquid Chromatography (FPLC), using a gradient of 200 mM Tris buffer for binding and 200 mM Tris buffer with 1 M NaCl for eluting.

Ferroxidase activity assay and further purification.

Fractions with high UV-absorbance at both 350 nm and 280 nm were selected and tested with FereneS (3-(2-Pyridyl)-5,6-di(2-furyl)-1,2,4-triazine- 50,500-disulfonic acid disodium salt, Sigma Aldrich) or FerroZine™ (3-(2-Pyridyl)-5,6-diphenyl-1,2,4-triazine- 40,400-disulfonic acid, Acros Organics), which are Fe^{2+}-specific chelators used for colorimetrically measuring free Fe^{2+} concentration. FereneS forms a complex with Fe^{2+} with maximum absorbance at 600 nm while FerroZine™ forms a complex with maximum absorbance at 562 nm.

In order to test the activity, 10 µL of selected fractions were pipetted into a 96-well plate, with the addition of 140 µL 20 mM MOPS buffer containing 200 mM NaCl at pH 6.85. Then 30 µL 1 mM $FeCl_2$ was added to each fraction sample. From this mixture, 20 µL was taken out into a new plate containing 180 µL 1.7 mM FerroZine™ solution. After 15 min incubation at 37 °C,

20 µL of a 1.7 mM FerroZine^{TM} solution was added to each sample. Fractions with low absorbance at 562 nm (as measured with a SpectraMax i3x instrument (Molecular Devices) and compared to a buffer control where no protein is present) indicate the presence of ferroxidase activity and are considered active fractions.

Active fractions (showing Fe^{2+} uptake activity) were pooled together. Pooled fractions were further purified by gel filtration with Superdex 200 16/60 HiLoad column using 20 mM MES buffer with 150 mM NaCl at pH 6.5 (De Meulenaere *et al.*, 2017). Protein concentration was determined by performing Bradford assay and diluted with 20 mM/ 200 mM MOPS buffer containing 200 mM NaCl at pH 6.85 to the desired concentration for each specific experiment involving ChF. ChF solutions were stored at room temperature.

Fe-binding Protein Identification with FPLC

We performed this step by using different types of affinity columns to specifically target iron-related protein in the mucus.

Fe^{2+} -affinity column.

Based on the fact that *C. variopedatus* photoprotein utilizes Fe^{2+} as cofactor, we intend to use Fe^{2+} as a "bait" to fish out the photoprotein. Therefore, we used an immobilized metal ion affinity column— "Hi-Trap Chelating HP" column in an attempt to extract Fe^{2+}-binding protein in the worm mucus. In an attempt to find the optimal buffer system where Fe^{2+} is most stable, Fe^{2+} stability was tested in different buffers using colorimetric assay (with 1 mM FereneS). After comparing Fe^{2+} stability in sodium acetate, sodium phosphate and MES buffer at pH 5.5, MES

buffer system was chosen to carry out the chromatography in ÄKTA FPLC system at 4 °C because this kept Fe^{2+} stable for the longest time. The 'Competitive Elution' method, specified in the manufacturer's manual (GE Healthcare), was carried out with the following MES buffers listed in Table 1.

Table 1. Buffers used in Fe-affinity column

Binding Buffer	0.02 M MES 0.5 M NaCl pH 5.5
Elution Buffer	0.02 M MES 0.5 M NH_4Cl pH 5.5
Stripping Buffer	0.02 M MES 0.5 M NaCl 0.05 M EDTA pH 5.5

Mucus from 4 worms was extracted with the addition of 9 mL MES binding buffer in a plastic reservoir. The extracted material was filtered with a syringe filter with 0.45 μm pore size (Whatman). Half of the filtrate (~5 mL) was prepared for the column (fresh mucus) while the other half was frozen in -20 °C (frozen mucus) for a comparison run the next day. Following steps on the manual, 0.1 mM $FeCl_2$ solution was loaded onto the column, mucus sample was injected, then washed with binding buffer for 5 column volumes, and lastly, eluted from the column using a continuous gradient. Eluted fractions were collected in volumes of 0.1 mL. Afterwards, the column was stripped clean with Stripping Buffer. The same process was repeated on the frozen mucus the next day.

Fractions of fresh and frozen mucus containing protein peaks (at 280 nm) were visualized on a Bolt™ Bis-Tris Plus 4-12% SDS-PAGE gel. Fractions of identical protein compositions were pooled and concentrated down to 1 mL by centrifuging in Amicon® centrifuge tube Ultra-4 (3 kDa) at 3820 ×g at 16 °C.

Cation-exchange column

In order to achieve better separation of the protein mixture from the Fe-chelating column, cationic exchange with HiTrap IEX-SP Sepharose XL column was performed with the previously concentrated fractions using buffers in Table 2.

Table 2. Buffers used in cationic exchange column

Starting Buffer	0.02 M sodium acetate pH 4.0
Elution Buffer	0.02 M sodium acetate 1 M NaCl pH 4.0

The concentrated fresh and frozen mucus eluted fractions (1 mL) were respectively run through the SP sepharose XL column, washed with starting buffer and eluted with a continuous gradient changing from 0% to 100% elution buffer in 20 min. Eluted fractions were collected in volumes of 0.1 mL. SDS-PAGE and Native-PAGE was used to visualize the degree of separation from the column. In the case of Native-PAGE, Novex^{TM} tris-glycine 4-20% gel was utilized as well as hand-cast 10% native gel following the recipe in Surecast^{TM} manual.

Mucus luminescence test with metal ions

We know that the mucus luminescence uses iron as a co-factor and that ferritin seems to play a critical role in fueling energy to the light production. My interest was therefore to look at dose-response of alternative co-factors but also ferritin-inhibitors on the light production.

Fe^{2+}-dose response

In an attempt to establish a Fe^{2+} concentration-light production dose response curve, we tested the mucus with $FeCl_2$ solution of a range of concentration from 0.001 mM to 10 mM. 500 µL mucus was extracted from a single worm and diluted to a 1/3 concentration with 1 mL milliQ (mQ)

water. It is necessary to take the effect of dilution into consideration because we observed that when add mQ water is added to the freshly extracted mucus, light production will increase. Usually the light production reaches maximum when the mucus is diluted 3-4 times. Therefore, in order to keep a standard baseline, injections are conducted on 3-times-diluted mucus in order to rule out the effect of dilution.

In a white opaque 96-well plate, 50 µL aliquots of the diluted mucus were pipetted into wells. In the SpectraMax i3x (Molecular Devices), a spectrophotometer, initial mucus light production—luminescence kinetics—was measured over 10 min with a measurement interval of 30 s. Then, as fast as possible, 50 µL $FeCl_2$ solution of 7 different concentration (in addition to mQ water as a negative control)—0.005 mM, 0.01 mM, 0.05 mM, 0.1 mM, 1 mM, 2 mM, 10 mM—was added into the 8 rows of mucus samples with 3 repeats of each experimental group. Luminescence kinetics was monitored again for 10 min. This experiment was repeated in triplicate on a total of 10 individual worms.

Effect of Co^{2+} and Zn^{2+} on mucus bioluminescence

Fresh mucus (500 µL) was extracted and diluted with 1 mL mQ water. Several 50 µL aliquots were pipetted into a white opaque (side walls, to optimize light collection) 96-well plate (bottom plate was transparent). In the SpectraMax spectrophotometer, background luminescence of mucus without any additions was measured for 10 min. Then, 50 µL of 0.01 mM, 0.1 mM, 1 mM $CoCl_2$, and 0.01 mM, 0.1 mM, 1 mM $ZnCl_2$ was injected (in addition to mQ as negative control), repeating in triplicates. After monitoring luminescence for 10 min, 100 µL 0.01 mM

$FeCl_2$ was added subsequently to each sample. Then luminescence kinetics was measured for another 10 min. Immediate effect on light production was compared between two injections.

Effect of metal ion on ChF Fe^{2+} Uptake Activities

Ferrous iron uptake activity test

To further confirm the assumption that Zn^{2+} blocks ferritin activity while Co^{2+} does not affect ferroxidation, eight aliquots of ferritin solution were prepared by adding 80 µL MOPS buffer (0.2 M MOPS 0.2 M NaCl pH 6.85) to 20 µL 1 mg/mL ChF. Different concentrations of $ZnCl_2$, $CoCl_2$, and $FeCl_2$ solutions were prepared according to the ChF concentration for each ferritin cage to have 100 Zn^{2+}, 2000 Zn^{2+}, 100 Co^{2+}, 2000 Co^{2+}, 100 Fe^{2+}, 2000 Fe^{2+} molecules, in addition to negative controls shown in the table on the right. 200 µL of each of these metal solutions were incubated with 1 mg/mL ChF at 37 °C for 1 h respectively.

Table 3. Metal Ion incubation with Chaetopterus ferritin

ChF + 100 Co^{2+} each cage
ChF + 2000 Co^{2+}
ChF + 100 Zn^{2+}
ChF + 2000 Zn^{2+}
ChF + 100 Fe^{2+}
ChF + 2000 Fe^{2+}
ChF + mQ
MOPS buffer + mQ

Afterwards, in a 37 °C water bath, 300 µL of 0.5 mM $FeCl_2$ was pipetted into the samples. 20 µL aliquots were transferred into 96-well plate with 140 µL 1.7 mM Ferrozine solution (an equivalent to FereneS) in each well at time points 0, 2, 4, 6, 8, 10, 12, 14, 16, 18, 20, 25, 30, 35,

40, 45, 50, 55, 60 min. Absorbance at 562 nm was then measured in SpectraMax™ i3x (Molecular Devices®).

Co^{2+}-affinity column

In the FPLC machine, "HiTrap Chelating HP" column was utilized to perform Co^{2+} affinity chromatography on the mucus to compare with the result from the Fe^{2+} affinity column. The following buffers in Table 4. were used during the process. Around 2 mL of mucus was extracted and pooled from 4 worms, then equal amount of 2× buffer stock was added to dilute the sample. Syringe filter with 0.45 μm pore size (Whatman) was used to filter the mucus solution.

Table 4. Buffers for Co-Affinity column

2× Buffer Stock	0.04 M 1 M NaCl pH 7.44
Binding Buffer	0.02 M sodium acetate 0.5 M NaCl pH 7.44
Elution Buffer	0.02 M sodium acetate 0.5 M NaCl 1 M imidazole pH 7.44
Stripping Buffer	0.02 M MES 0.5 M NaCl 0.05 M EDTA pH 7.44

Following the manufacturer's manual, 0.5 mL 0.1 mM $CoCl_2$ in mQ was loaded onto the column. Afterwards the filtered mucus solution was pumped through the column from the sample loop, then binding buffer was used to wash out any unspecific bindings. Eventually a buffer gradient was set up as 0%-50% elution buffer in 20 min, and afterwards to 100% in 10 min for gradually increasing imidazole concentration and slowly eluting the bound proteins. Fractions were collected in volumes of 0.5 mL. Co^{2+} ions were stripped from the column by 10 mL of stripping buffer.

Effect of chromatography fractions on mucus luminescence

If the eluted fraction from FPLC contains the photoprotein, or any protein that is involved in the light production mechanism, back adding the fraction to the complete original reaction

complex should cause an increase in light production. Therefore, in the luminometer, we monitored light level change when fractions from the Co^{2+}-affinity chromatography were added back to the mucus. Background light of 50 µL 1/3 diluted mucus was measured for 30 s, then same volume of obtained fractions from the FPLC was injected manually to the mucus. Subsequent light production was monitored for another 30 s.

Data processing

Collected data were organized in Excel and plotted using boxplot as well as the regression functions in MATLAB.

In the section where we wanted to look for relationship between light production before and after Fe^{2+} injection, sum before is plotted against sum after in log scale in MATLAB. Points were scattered based on different Fe^{2+} injection concentrations in log scale because each mucus' ability to produce light differs greatly. A linear relationship in log scale between light before addition and light after injection converts to $y = x^k \bullet 10^b$ format relationship in normal scale. The line y = x in log scale was plotted for comparison of change in light production. R-square values were calculated to estimate the goodness of fit.

Results

My project was successful in extraction of a Fe^{2+} binding protein from the mucus complex. In order to create a standard for future experimenting, we have discovered a preliminary stimulation-inhibition curve of Fe^{2+} concentration and mucus bioluminescence. By injecting Co^{2+} and Zn^{2+} in addition to Fe^{2+} into the mucus, we were able to reject the hypothesis that ferritin

participate in a redox chain reaction to power the bioluminescence. Last but not least, by using Co^{2+} affinity column, we purified a light-inducing protein from the mucus complex.

Fe^{2+}-binding protein extraction with FPLC

Fe^{2+}-binding protein was extracted from the Fe^{2+}-affinity column

According to the SDS-PAGE visualization of FPLC fractions in Figure 5, multiple proteins in the worm mucus were eluted from the Fe-binding column. The most abundant protein occurs at a size of around 30 kDa. On the gel, it seems like this protein band consists of 2-3 smaller bands that are close in size. This pattern also occurs at around 70 kDa and 140 kDa, which indicates that these three bands are likely one protein that consists of different numbers of subunits. It is also obvious that fresh and frozen mucus do not differ in composition. However, adding these fractions back to the mucus does not result in increase in light production, even after buffer exchange to a more neutral pH.

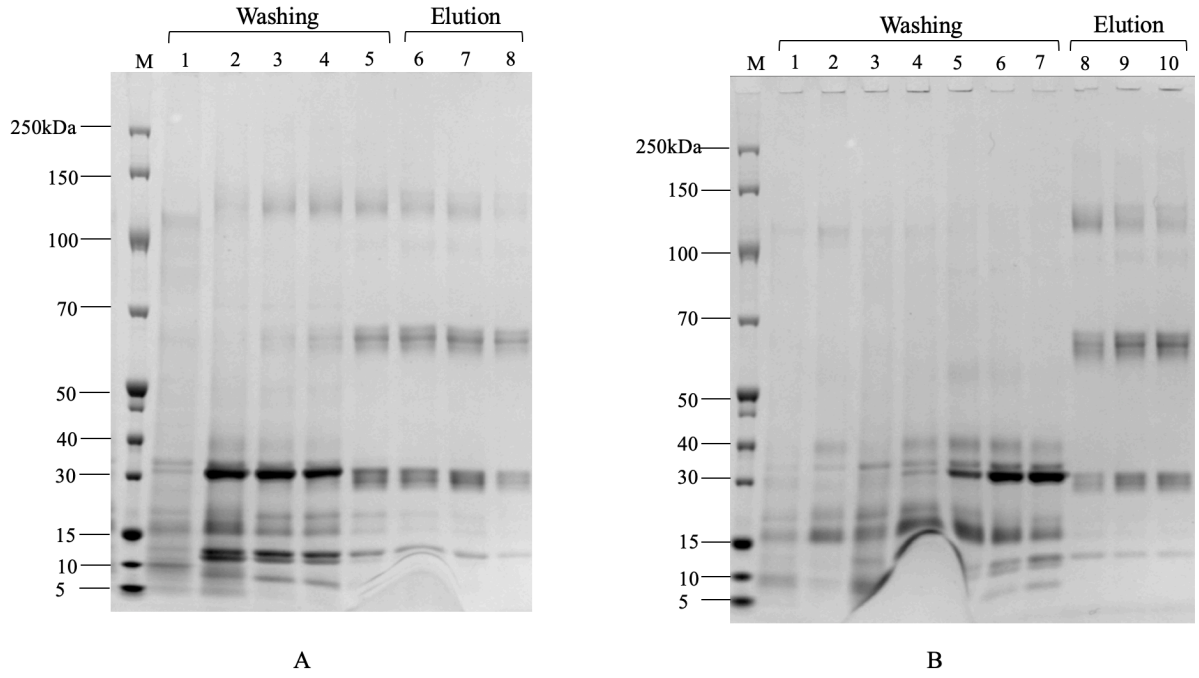

Figure 5. SDS-PAGE gel of mucus fractions from the Fe^{2+}-Chelating column. A: fractions from fresh mucus. B: fractions from frozen mucus. Washing and elution fractions from the column were indicated on top of the image. "M" represents the protein marker. Proteins of size ~30 kDa, 70 kDa and 140 kDa were washed and eluted from the column from both fresh and frozen mucus sample.

Cation-Exchange column was not able to separate the three subunits of Fe^{2+}-binding protein extracted

In order to further separate the smaller bands in each subunit, the elution peak fractions were combined, concentrated and run through HiTrap IEX- Sepharose XL column. The resulting separation presented Figure 6 indicates that the separation of smaller bands in each lane (at around 30 kDa and 60-65 kDa) is not achieved through the cationic exchange column. Since the protein profile still shows that the smaller bands are not separated, which is almost identical compared to the elution fractions from the Fe-chelating column in Figure 5.

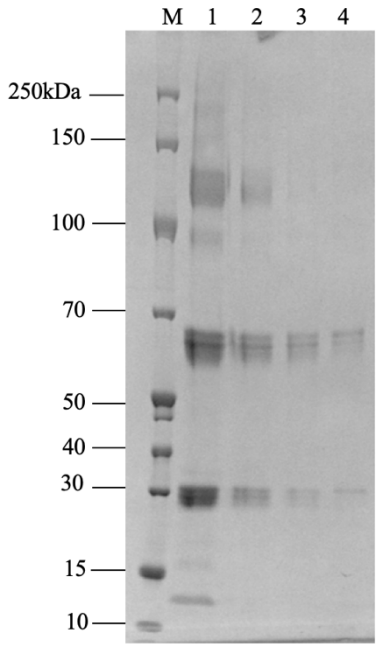

Figure 6. SDS-PAGE of fresh and frozen mucus fractions from SP XL column. The lane labelled "M" is the molecular standard used on this gel—PageRuler Broad Range Unstained (Thermofisher). Lane 1 is concentrated peak from Fe affinity column as a comparison, while 2 to 4 are fractions from the cationic exchange protein peak.

Mucus luminescence test with metal ions

Fe^{2+}-mucus luminescence test reveal an stimulation-inhibition dose response curve

As shown in Figure 7, injections of $FeCl_2$ solutions of different concentrations have different effects on the light production of the mucus sample. Comparing to the negative control of adding only mQ water to mucus, where light level stayed relatively stable, Fe^{2+} concentration has an stimulation-inhibition dose response on the production of light. When added Fe^{2+} concentration is less than 0.1 mM, the effect from iron is stimulating. When at 0.1 mM, the effect is similar compared to adding mQ water. Once the added concentration begins to increase to above 0.1 mM, a light-inhibiting effect is observed.

In order to include data points from multiple worms and normalize the difference in the initial light production of mucus extracted from different worms, we first took the sum of the last

5 points before and the first 5 points after injection of Fe^{2+} solution as illustrated in Figure 8. We define a new parameter, $\frac{sum\ after - sum\ before}{sum\ before}$ (Light Change Ratio, **LCR**), in this case to represent each repeat from a single worm in a scatter plot. When LCR value is larger than 0, where sum after is larger than sum before, it represents a light-stimulating event. The data from 10 worms were represented in a boxplot in Figure 9, showing that the pattern of a stimulation-inhibition dose response is consistent among the mucus produced by different worm individuals.

In Figure 10, sum before is plotted against sum after. We fitted the function $y = x^k \cdot 10^b$ to the data and presented in log scale. The line y = x in log scale was plotted for the comparison of change in light production. According to the R-square values, the fitness of regression is relatively high in all cases. The data showed us a consistent linear relationship present in logarithmic scale—an exponential function when converted to normal scale—regardless of the effect of Fe^{2+}.

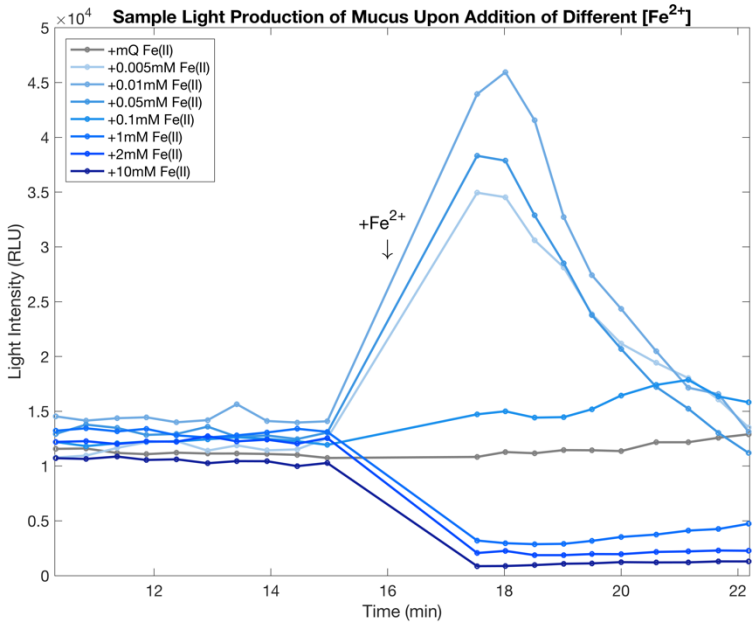

Figure 7. Light production of mucus from a single worm before and after the addition of $FeCl_2$ and mQ as a negative control. $FeCl_2$ solution was injected manually at the time point shown where the arrow indicates. Different concentrations of $FeCl_2$ solution was added volume-to-volume to 1/3 diluted mucus.

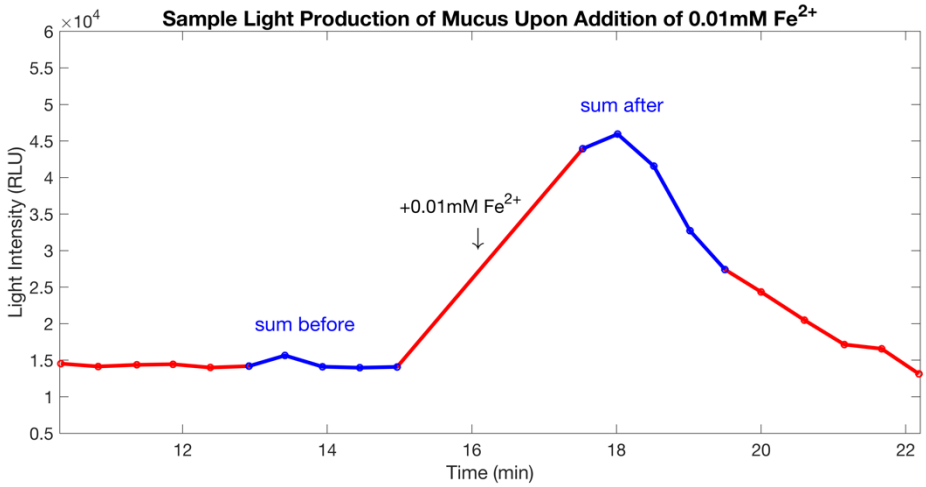

Figure 8. A sample light production curve illustrating the summation calculations. Five points before and after $FeCl_2$ injection were summed up as "sum before" and "sum after", respectively, to perform further comparisons between individual mucus samples.

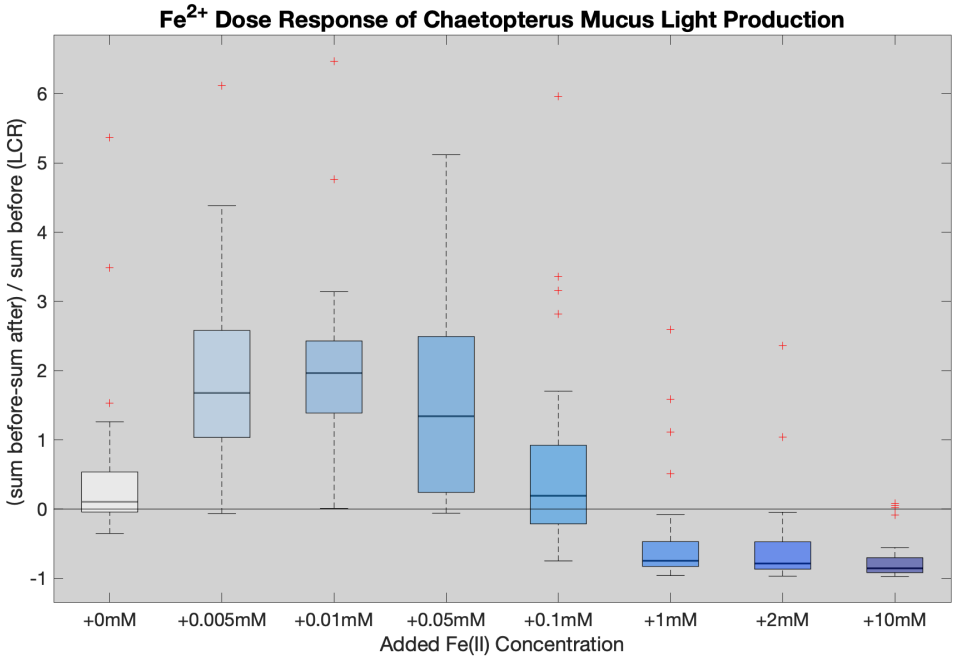

Figure 9. Boxplot of LCR for all 3 repeats of adding each concentration of $FeCl_2$ performed on a total of 10 worms' mucus. Darker shades of blue correspond to higher concentrations of $FeCl_2$ added. A datapoint lower than 0 represents a decrease in light while a value larger than 0 stands for inhibition. Each value in the boxplot is standardized by division of sum before, which differs because of the variation in initial light production of worm individuals.

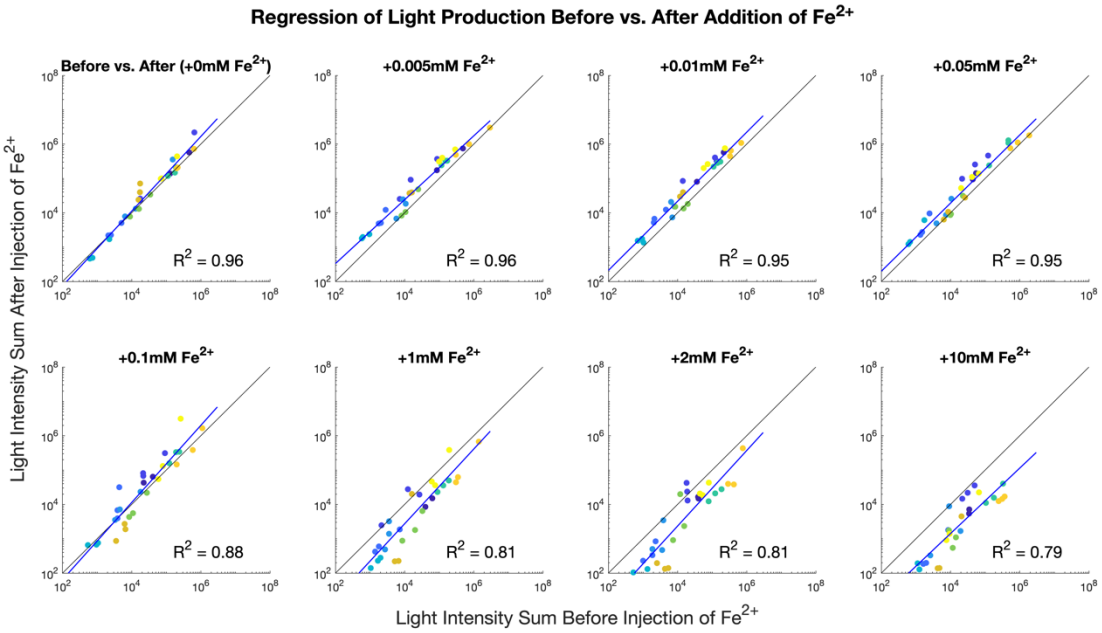

Figure 10. Regression of sum before vs. sum after in log scale fitting the equation $y = kx + b$ ($y = x^k \cdot 10^b$ in normal scale). Blue line is the line of best fit in comparison to $y = x$ (black line). R^2 value of each regression was calculated and labeled on the graph. When light production is potentiated, the best fit line should be above $y = x$; when light production is inhibited, blue line should be below $y = x$.

Zn^{2+}inhibits mucus bioluminescence temporarily while Co^{2+}has permanent inhibition

The effect of Co^{2+} and Zn^{2+} was tested in comparison to Fe^{2+}. In Figure 11, injection on a sample from a single worm and the resulting light production change was shown. Concentrations of 0.01, 0.1 and 1 mM were chosen according to Figure 9, where the corresponding Fe^{2+} concentration is stimulating, unchanging and inhibiting light production. In this particular sample, injection of Co^{2+} and Zn^{2+} seem to have an instantaneous inhibiting effect. Afterwards, 0.01 mM Fe^{2+} was added to test if the entire reaction is blocked by Co^{2+} or Zn^{2+}, because this injected concentration was proven to stimulate mucus light production to the greatest extent (Figure 9).

In order to take all 10 worm mucus sample into consideration, $\frac{sum\ after - sum\ before}{sum\ before}$ value (LCR), calculated from value of five points respectively, was used to represent the change. Only

in this case we have three LCR values in each test in order to monitor the light production curve more thoroughly after injections (Figure 12). According to the boxplot obtained (Figure 13), when looking at the first injection only, as Co^{2+} injection concentration increases, an inhibitory effect become more significant—conforming to a dose response model. A similar trend appears in the case of Zn^{2+} injection, but the increasing inhibitory effect with more concentrated Zn^{2+} injected is more significant.

When the injection of 0.01 mM Fe^{2+} happens after the previous injection, in samples where Co^{2+} is injected, Fe^{2+} can no longer stimulate light in mucus. The reaction is repressed to a larger extent in samples where more Co^{2+} is added. This means that Co^{2+} is blocking the reaction, or a certain part of the light production reaction chain. In the case of Zn^{2+}, when Fe^{2+} is added to the reaction, light production is restored. Light production restoration increases with the concentration of Zn^{2+} in the previous injection. Zn^{2+} could be temporarily blocking the photoprotein in the absence of Fe^{2+}, but out competed by Fe^{2+} once iron come into presence.

In order to investigate whether Zn^{2+} and Co^{2+} are blocking the reaction because of blocking the *Chaetopterus* ferritin core or channel, an Fe^{2+} uptake experiment was conducted on ferritin with the presence of Zn^{2+} and Co^{2+} of high (2,000 ions per ferritin cage) and low (100 ions per cage) concentration. According to Figure 14, compared to the negative control where no ferritin is present in the buffer, presence of high concentration of Zn^{2+} hinders the Fe^{2+} uptake ability of ferritin.

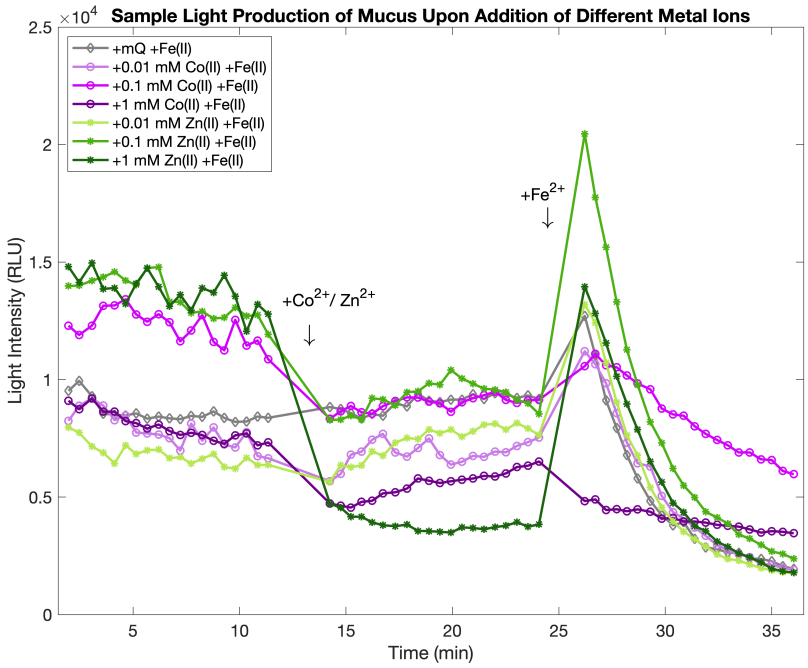

Figure 11. Sample time series of mucus (from a single worm) light production upon the injection of first Zn^{2+} / Co^{2+} and then Fe^{2+} as shown by the arrows. Three different concentration of $ZnCl_2$ and $CoCl_2$ was injected while $FeCl_2$ concentration was fixed at 0.01 mM.

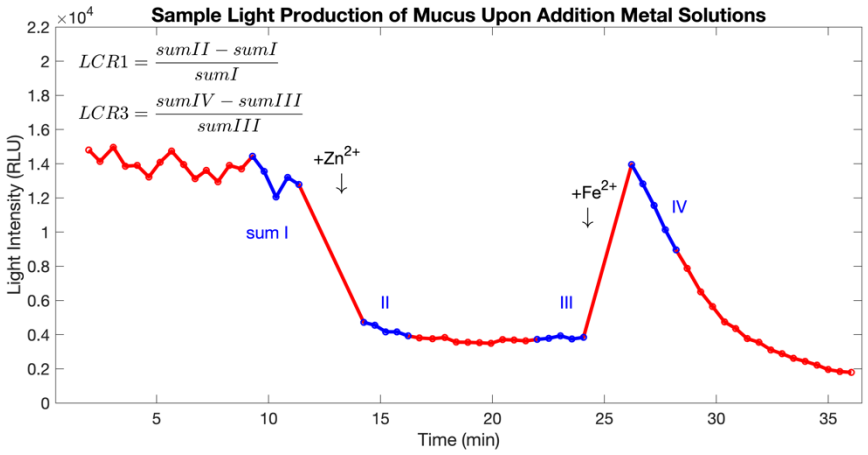

Figure 12. A sample light production curve of summation calculations. Five-point summations were calculated at the initial point of measurement (sum I), before Co^{2+}/Zn^{2+} injection (II), after first injection (III), before (IV) and after (V) injection of ferrous iron, and the end phase of measurement (VI). Five LCR values can be calculated from these six sum values. For example, LCR1=(sumII-sumI)/sumI, LCR2=(sumIII-sumII)/sumII, LCR3=(sumIV-sumIII)/sumIII.

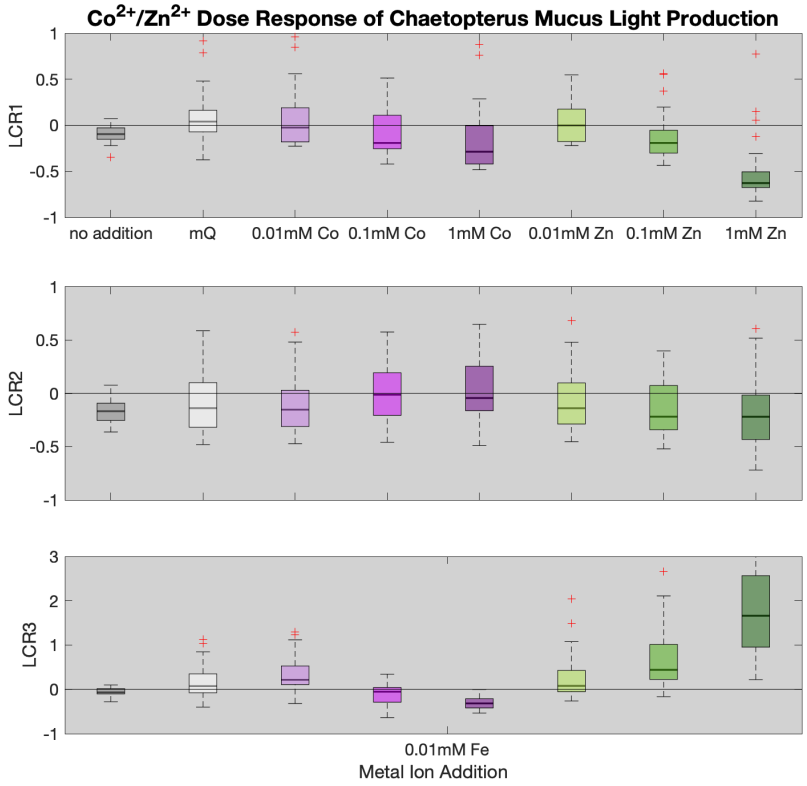

Figure 13. Boxplot of LCR values of mucus when adding each metal solutions. Three consecutive LCR values were plotted and labelled. Effect of Co^{2+}/ Zn^{2+} and consecutive Fe^{2+} injections on mucus light production. Darkening shades of purple/green represents increasing concentration of $CoCl_2$ /$ZnCl_2$ injection. $FeCl_2$ injection concentration was fixed at 0.01 mM. (Figure 9.). LCR1 describes the effect of the first injection consisting of either Co^{2+} or Zn^{2+}; LCR2 represents the light production trend after the first injection; LCR3 stands for the effect of adding 0.01 mM Fe^{2+}.

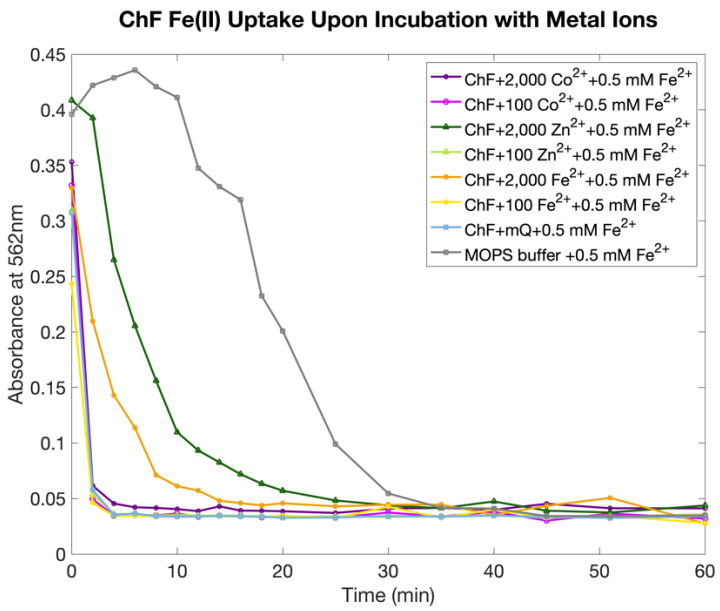

Figure 14. ChF Fe^{2+} uptake in the presence of high (2,000 ion per ferritin cage) and low (100 ion per ferritin cage) level of Zn^{2+} and Co^{2+}. Absorbance at 562 nm represents the concentration of ferrozine-Fe^{2+} complex, which represents the concentration of free Fe^{2+} in the solution.

Co^{2+} -affinity column renders light-enhancing protein from mucus

From the SDS-PAGE of Co-Affinity column fractions (Figure 15), there is a pronounced protein band at around 37 kDa and a relatively faint band at 17 kDa in the eluted protein peak fractions from both repeats. Then the eluted fraction was added back to the mucus in the luminometer and tested for light change. Figure 16 presents two independent repeats of Co^{2+}-affinity chromatography in the FPLC machine. Compared to the buffer control where no protein is present (a and c), an increase in light production always occurs when the eluted fraction is added to the mucus (b and d).

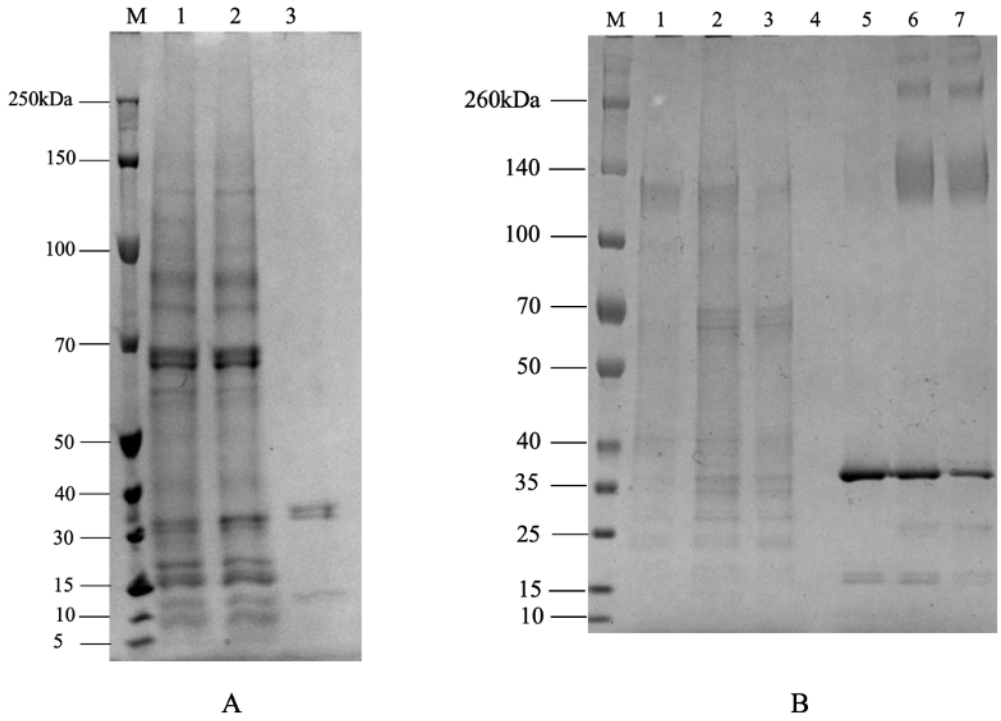

Figure 15. SDS-PAGE of fractions from two repeats of Co^{2+}-affinity column. "M" lane is where protein marker is located. A: lane 1-2 are wash fractions and 3 is eluted fraction by approximately 2% elution buffer containing imidazole. B: lanes 1 to 3 are the wash fractions. Lanes 5-7 are eluted fractions. An obvious protein band shows up at a size between 35 and 40 kDa. Faint protein bands were also located at 25 kDa and 15 kDa.

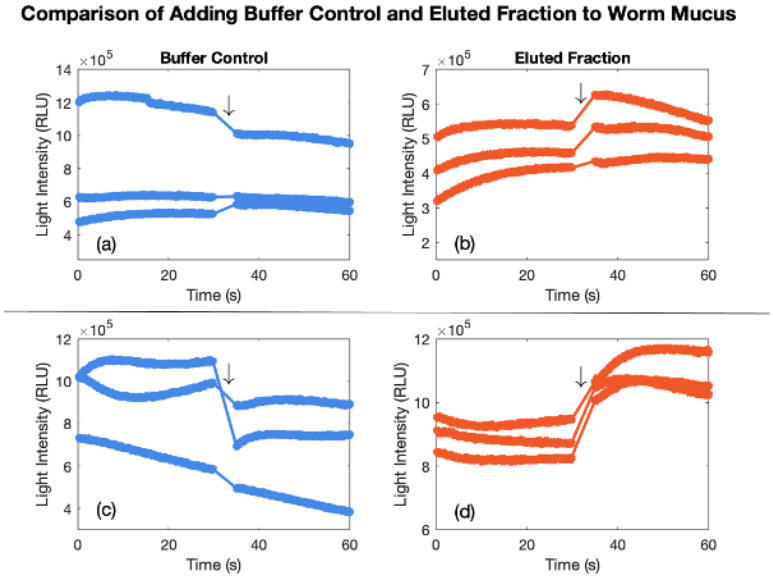

Figure 16. Light production of adding buffer control to mucus vs. adding eluted fraction to mucus from 2 independent repeats (A and B corresponding to Figure 13). The three curves in each graph represent 3 repeats of the same injection.

Injections are shown by downward arrows on the graph. Blue curves are negative controls with injections containing only buffer background; red curves are injections containing the eluted protein.

Discussion

A variety of data was collected during the project, I organized the information gathered together from different experiments to further understand the mechanism of light production

Mucus luminescence shows a stimulation-inhibition dose response with Fe^{2+} concentration

In the case of aequorin, it was first proven that the relationship between concentration of Ca^{2+} and the protein follows a typical dose response curve, when a higher concentration of Ca^{2+} is added to aequorin, the light production of aequorin first increases at a logarithmic speed and then approaches saturation where light production is flattened out (shown in Fig. 1. in Blinks *et al.*, 1976).

We investigated the relationship between ferrous iron concentration and mucus light production and found that the result is quite different from aequorin. We observed a stimulating effect on light production when Fe^{2+} injected is lower than 0.1 mM, as the injection concentration increases from this point, an inhibition is observed. This response is different from the aequorin-Ca^{2+} relationship in that as the concentration of cofactor reaches a certain threshold, the inverse effect will occur. An alternative explanation for the difference could be that, in Fig. 1. of Blinks *et al.* (1976), the cofactor concentration (Ca^{2+}) range tested (10^{-4} mM to 10^{2} mM) is wider than that we did with Fe^{2+}. Therefore, we can conclude that the *Chaetopterus* photoprotein in the mucus behaves differently with its metal cofactor compared to traditional photoprotein. However, since at this stage, it is very difficult to quantify the photoprotein concentration in each raw mucus sample, our estimation of the dose response curve it still preliminary. It would be ideal if in the

future we can isolate the photoprotein from the complex. The reason why high concentration of Fe^{2+} inhibits light production is not understood currently. We infer that high concentration of free Fe^{2+} can catalyze the production of reactive oxygen species (ROS) through Fenton reaction (Toyokuni, 1996). ROS is destructive because of their unpaired electrons, which can attack many biological components in the mucus and damage the light production pathway. We attempted to understand the mechanism more using other metal ions (Co^{2+} and Zn^{2+}) in the following section.

Another interesting aspect of the mucus luminescence is that no matter inhibited or stimulated by Fe^{2+}, light production before and after iron addition follows a linear trend in log scale. This phenomenon indicates that light before (x) and after injection (y) of the worm mucus are always linearly related in log scale ($y = kx + b$) —exponentially related in normal scale ($y = x^k \cdot 10^b$, k and b corresponds with the slope and intercept from linear function obtained in log scale). Mucus from different worms varies greatly in their ability to produce light. We can infer that each worm mucus potential light production ability is positively related to its initial bioluminescence level. From this point forward, we see a possibility to establish a model for the mucus light production. It is possible to increase our sample size and construct a more complete curve of light production before and after Fe^{2+} injection, so that we can make predictions of and perhaps manipulate light production under different circumstances based on the initial light level of a mucus sample by controlling the amount of Fe^{2+}.

Co^{2+} and Zn^{2+} are competitive inhibitors with different affinities

Based on what is already known in the literature, Co^{2+} is able to participate in a similar reaction inside of the ferritin cage compared to the reaction of Fe^{2+}, in that Co^{2+} can be converted

by horse spleen ferritin into a Co^{3+}-oxyhydroxide (Douglas & Stark, 2000). If Co^{2+} can go through a similar redox reaction with iron, relating back to the hypothesis brought up in 2016—the reaction between Co^{2+} and ferritin should also be able to generate electrons that can push forward the redox chain which ultimately powers the production of light (Rawat & Deheyn, 2016).

On the other hand, Zn^{2+} was known to be the inhibitor of ferritin's ferroxidase activity. Treffry *et al.* demonstrated in their 1998 paper that Zn^{2+} and Fe^{2+} bind to the same site inside of the ferritin cage, and Zn^{2+} is an inhibitory competitor on Fe^{2+} because it blocks the reaction site and prevent more Fe^{2+} from reacting. In this case, if ferritin's ferroxidase activity plays a part in the mucus luminescence and Zn^{2+} can inhibit this activity, then adding Zn^{2+} to the mucus should inhibit light production.

Our experiments testing the ChF activity matches the statements in the literature, the presence of high concentration of Zn^{2+} (approximately 2,000 Zn^{2+} ions per ferritin cage) slows down the uptake of Fe^{2+}. While the presence of Co^{2+} does not interfere with ferritin's normal activity. Correlating ferritin activity with mucus bioluminescence, we turn to the investigation of the effects of these metal ions on light production, small amount of Co^{2+} ($\leq$ 0.01 mM) added (volume to volume) to the mucus does not affect the luminescence pathway because light can be restored by adding Fe^{2+} again. However, as addition concentration increases, the reaction pathway is gradually blocked by Co^{2+}. In comparison, the bioluminescence is temporarily inhibited by addition of increasing concentrations of Zn^{2+} but can be restored by addition of Fe^{2+}. Therefore, the ability of mucus to produce light is not impeded by Zn^{2+} because when the bioluminescence is more inhibited in the first place, light can be restored to a relative larger extent by the subsequent presence of Fe^{2+}.

These results appear to be the opposite of the statements that we made. Co^{2+} can be oxidized by ChF but performs an inhibition on bioluminescence, while Zn^{2+} blocks ferritin but not the light producing reaction pathway. We infer that the key role of interaction in this case lies in metal ions and photoprotein, instead of ferritin. We can conclude from our result that Co^{2+} and Zn^{2+} are both competitive inhibitors for the ferrous iron binding site on photoprotein. However, Co^{2+} has a stronger affinity for binding compared to Fe^{2+}, while Zn^{2+} has a lower binding affinity. This is why when Fe^{2+} is added to the system again, it can successfully outcompete Zn^{2+} with binding to photoprotein but failed in the case of Co^{2+}.

Instead of focusing on one single protein component of this reaction "black box", we should take the entire system into consideration and keep in mind that this process involves more than a single protein. In the future, it will be ideal if we can identify and purify each component from the reaction pathway and re-adding them back together to see if light can be re-created *in-vitro*.

Iron-binding proteins were found in the luminous mucus

Evidence from the FPLC indicates that there are indeed proteins present in the mucus that bind to the Fe^{2+} on the column. The protein band at around 30 kDa from the elution fractions seem to occur in the form of 3 protein bands that are closely related in size. Together with bands at 60-65 kDa and 120-130 kDa, these are possibly the same protein consisting of unseparated subunits because they have a similar triple-band pattern. Separation of these bands utilizing cationic exchange chromatography has proven to be ineffective. This means that the closely located bands at 30 kDa are strongly attached to each other. We can exclude the fact that this protein is ferritin

because the size of ferritin subunits lies in the 20-23 kDa range. Thus, these protein bands are very good candidates for photoprotein because they exhibit an iron binding property. However, combining these fractions to the complete mucus complex does not result in light increase even after we exchanged the fraction buffer to a more neutral pH at 6.85, as expected of photoprotein.

We cannot rule out the possibility that what we obtained from the column is the photoprotein, but it is possible that the photoprotein is denatured on the Fe^{2+}-Affinity column where a low pH is required to prevent the oxidation of ferrous iron to ferric iron, and was irreversibly denatured even though buffer exchange was performed. However, it should not be the main possibility because the protein bands did not turn into a smear on the gel. It is also possible that the chemical environment of the buffer is disrupted by the large amount of hydrogen ions present at low pH (equilibrium of charges pushed to the extreme of the balance). In addition to that, the three closely located bands make the extraction of a single protein from gel very difficult, which creates an obstacle for protein sequencing where high purity is required. Therefore, we need to seek an alternative to replace the low-pH affinity column to see if we can obtain light-stimulating fractions.

Using Co^{2+} as a substitute cofactor, we demonstrated that we isolated a good candidate to be the mucus photoprotein

As we demonstrated in our previous section, Co^{2+} is a competitive inhibitor that binds to the photoprotein with even higher affinity than the binding of Fe^{2+}. Therefore, we believe that Co^{2+} can be utilized as a substitute cofactor for photoprotein. This characteristic makes us see the possibility to use Co^{2+}-affinity column to purify the Fe^{2+}-binding protein. One benefit of Co^{2+} is that it is not as easily oxidized compared to Fe^{2+}, and does not require a low pH for maintaining

oxidation state stability. Therefore, we can run the column directly at pH 7.44, which is closer to that of sea water and better for the conservation of protein conformation.

What we obtained from the column is a significant protein band at around 35 kDa, together with faint bands at 17 kDa and 25 kDa. Recombining the eluted fraction with the mucus results in an increase in light production in both repeats. Comparing the results, it is reasonable to infer that either the 35 kDa protein or 17 kDa protein plays a part in the bioluminescence of *C. variopedatus* mucus. The photoprotein, aequorin, extracted from *Aequorea* has a size of 22 kDa, while obelin is 20 kDa. *Renilla* luciferase is 36 kDa in size. Therefore, what we can conclude here is that the eluted protein on our gel is in the size range of marine luciferases, but we cannot confirm without more molecular-level evidence. Our next step is to send out the protein bands for N-terminal sequencing. Once we have partial amino acid sequence of the proteins, we can go ahead and design primers for further detection of the gene in the worm RNA. Afterwards we will hopefully obtain the entire gene sequence and blast it against National Center for Biotechnology Information database.

Conclusion

In this project, our goal is to investigate the function of ferritin in the bioluminescence of *C. variopedatus,* as well as looking for the photoprotein. Fortunately, we are able to make promising progress on both aspect by taking advantage of the cofactor, Fe^{2+}, and other metal ions.

Our investigation on the relationship between Fe^{2+} concentration and light production of mucus leads us to the conclusion that light production and ferrous iron concentration follows an stimulation-inhibition dose response—Fe^{2+} stimulates light when under the threshold of 0.1 mM

injected but inhibits light production when threshold is exceeded. However, regardless of stimulation or inhibition, the light level of mucus before and after the injection of Fe^{2+} follows linear relationship in log scale. In an attempt to discover the effect of Co^{2+} and Zn^{2+} in comparison to Fe^{2+}, our results show that Co^{2+} and Zn^{2+} both do not stimulate light production at lower concentration (0.01 mM) and impede light at a higher concentration (1 mM). Furthermore, Co^{2+} blocks the reaction completely while light can be restored following Zn^{2+}. Zn^{2+} and Co^{2+} are both competitive inhibitors for binding to the cofactor site on the photoprotein, but Co^{2+} exhibits a much higher affinity. Subsequent test on *C. variopedatus* ferritin demonstrates that Zn^{2+}, while present in a relatively high concentration (around 2,000 per ferritin cage), can block Fe-uptake by ferritin. In our attempt to use Fe^{2+}-affinity column to extract Fe^{2+}-binding proteins, although we did attain protein fractions, adding them back to the mucus did not result in any significant increase in light production, even after buffer exchange to a neutral pH. When we switched to use a Co^{2+}-affinity column instead to purify part of the reaction chain because of its similarity to Fe^{2+}, protein fractions containing which can potentially be the photoprotein were eluted. These fractions from the FPLC exhibit a protein band at around 37 kDa, as well as a faint band at 17 kDa. An excitatory effect on light production indeed occurred when they were added back to the mucus.

References

Archer, S., Djamgoz, M. B., Loew, E., Partridge, J. C., & Vallerga, S. (Eds.). (2013). Adaptive mechanisms in the ecology of vision. Springer Science & Business Media.

Berrill, N. J. (1928). Regeneration in the polychæt *Chætopterus variopedatus*. *Journal of the Marine Biological Association of the United Kingdom*, *15*(1), 151–158. https://doi.org/10.1017/S0025315400055594

Blinks, J. R., Prendergastt, F. G., & Allenn, D. G. (1976). Photoproteins as Biological Calcium Indicators. In *REVIEWS* (Vol. 28, Issue 1).

Bou-Abdallah, F., Arosio, P., Levi, S., Janus-Chandler, C., & Chasteen, N. D. (2003). Defining metal ion inhibitor interactions with recombinant human H- and L-chain ferritins and site-directed variants: An isothermal titration calorimetry study. *Journal of Biological Inorganic Chemistry*, *8*(4), 489–497. https://doi.org/10.1007/s00775-003-0455-6

Chang, Y.-Y., Li, H., & Sun, H. (2017). Immobilized Metal Affinity Chromatography (IMAC) for Metalloproteomics and Phosphoproteomics. *Inorganic and Organometallic Transition Metal Complexes with Biological Molecules and Living Cells*, 329–353. https://doi.org/10.1016/B978-0-12-803814-7.00009-5

Deheyn, D. D., Enzor, L. A., Dubowitz, A., Urbach, J. S., & Blair, D. (2013). Optical and physicochemical characterization of the luminous mucous secreted by the marine worm Chaetopterus sp. Physiological and Biochemical Zoology, 86(6), 702-715.

De Meulenaere, E., Bailey, J. B., Tezcan, F. A., & Deheyn, D. D. (2017). *First biochemical and crystallographic characterization of a fast-performing ferritin from a marine invertebrate*. *November*, 4193–4206.

Desideri, A., Stefanini, S., Polizio, F., Petruzzelli, R., & Chiancone, E. (1991). Iron entry route in horse spleen apoferritin: involvement of the three-fold channels as probed by selective reaction of cysteine-126 with the spin label 4-maleimido-tempo. FEBS letters, 287(1-2), 10-14.

Douglas, T., & Stark, V. T. (2000). *Nanophase Cobalt Oxyhydroxide Mineral Synthesized within the Protein Cage of Ferritin*. https://doi.org/10.1021/ic991269q

Enders, H. E. (1905). Notes on the commensals found in the tubes of Chaetopterus pergamentaceus. *The American Naturalist*, *39*(457), 37-40.

Granick, S. (1946). Ferritin: its properties and significance for iron metabolism. Chemical reviews, 38(3), 379-403.

Haddock, S. H. D., Moline, M. A., & Case, J. F. (2010). *Bioluminescence in the Sea*. https://doi.org/10.1146/annurev-marine-120308-081028

Jones, T., Spencer, R., & Walsh, C. (1978). Mechanism and kinetics of iron release from ferritin by dihydroflavins and dihydroflavin analogs. *Biochemistry*, *17*(19), 4011–4017. https://doi.org/10.1021/bi00612a021

Lankester, E. R. (1868). Preliminary Notice of some Observations with the Spectroscope on Animal substances. *Journal of Anatomy and Physiology*, *2*(1), 114–116. http://www.ncbi.nlm.nih.gov/pubmed/17230736

Lewis, J. C., & Daunert, S. (2000). Photoproteins as luminescent labels in binding assays. In *Fresenius' Journal of Analytical Chemistry* (Vol. 366, Issues 6–7, pp. 760–768). Springer Verlag. https://doi.org/10.1007/s002160051570

MacGinitie, G. E. (1939). The method of feeding of Chaetopterus. The Biological Bulletin, 77(1), 115-118.

May, M. E., & Fish, W. W. (1978). The UV and visible spectral properties of ferritin. Archives of biochemistry and biophysics, 190(2), 720-725.

Nicol, J. C. (1952). Studies on Chaetopterus variopedatus (Renier). III. Factors affecting the light response. *Journal of the Marine Biological Association of the United Kingdom*, *31*(1), 113-144.

Rawat, R., & Deheyn, D. D. (2016). Evidence that ferritin is associated with light production in the mucus of the marine worm Chaetopterus. *Scientific Reports*, *6*. https://doi.org/10.1038/srep36854

Shah, D. U., Vollrath, F., Stires, J., & Deheyn, D. D. (2015). The biocomposite tube of a chaetopterid marine worm constructed with highly-controlled orientation of nanofilaments. Materials Science and Engineering: C, 48, 408-415.

Shannon, R. D. (1976). Revised effective ionic radii and systematic studies of interatomic distances in halides and chalcogenides. *Acta crystallographica section A: crystal physics, diffraction, theoretical and general crystallography*, *32*(5), 751-767.

Shimomura, O., & Johnson, F. H. (1966). Partial purification and properties of the Chaetopterus luminescence system. Bioluminescence in progress, 495521.

Shimomura, O. (1985). Bioluminescence in the sea: photoprotein systems. *Symposia of the Society for Experimental Biology*, *39*, 351–372. http://www.ncbi.nlm.nih.gov/pubmed/2871634

Shimomura, Osamu. (1981). *A new type of ATP-activated bioluminescent system in the millipede Luminodesmus sequoiae* (Vol. 128).

Toyokuni, S. (1996). Iron-induced carcinogenesis: The role of redox regulation. In *Free Radical Biology and Medicine* (Vol. 20, Issue 4, pp. 553–566). Elsevier Inc. https://doi.org/10.1016/0891-5849(95)02111-6

Widder, E. A. (2010). Bioluminescence in the Ocean. *Science*, *704*(5979), 704–708. https://doi.org/10.1126/science.1174269

Wilson, T., & Hastings, J. W. (1998). Bioluminescence. In *Annu. Rev. Cell Dev. Biol* (Vol. 14). www.annualreviews.org